# Parallel elevational replacement of hosts and parasites in a highly susceptible songbird genus

Daniele L. F. Wiley[1,2], Jessie L. Williamson[1,3], Silas E. Fischer[4], Selina M. Bauernfeind[1], Henry M. Streby[4], Kathy Granillo[5], Christopher C. Witt[1,2], and Lisa N. Barrow[1,2]

[1]Museum of Southwestern Biology, University of New Mexico, 302 Yale Blvd NE, Albuquerque, NM 87131, USA

[2]Department of Biology, University of New Mexico, 302 Yale Blvd NE, Albuquerque, NM 87131, USA

[3]Department of Zoology and Physiology, University of Wyoming, 1000 E. University Ave, Laramie, WY 82071, USA

[4]Department of Environmental Sciences, University of Toledo, Wolfe Hall Room 1235, 3050 West Towerview Blvd., Toledo, OH 43606-3390, USA

[5]United States Fish and Wildlife Service, Socorro, NM 87801, USA; retired

*Corresponding author: Daniele L. F. Wiley, dwiley7@unm.edu

Address: Department of Biology, University of New Mexico, Castetter Hall 1480, MSC03-2020, 219 Yale Blvd. NE, Albuquerque, NM 87131, USA

ABSTRACT

Elevational replacement distribution patterns underpin montane diversity and reflect the interaction of both biotic and abiotic pressures, but the degree to which parasites exhibit elevational zonation remains unclear. Investigating infection patterns in related host species across elevational gradients can reveal whether parasites and hosts show concordant patterns of elevational turnover, potentially due to shared historical and ecological factors. Here, we assessed patterns of elevational replacement in haemosporidian parasite assemblages that infect three congeneric songbird species: Bell's Vireo (*Vireo bellii),* Gray Vireo *(V. vicinior),* and Plumbeous Vireo (*V. plumbeus*), each of which breeds across distinct elevations and habitats in the southwestern United States. We screened a total of 248 individuals using cytochrome *b* PCR and microscopy. We identified 19 haemosporidian haplotypes, including eight novel lineages. We found that each of the three vireo species exhibited high haemosporidian prevalence (55.0–86.2%), with nearly all infections from the genus *Haemoproteus* (subgenus *Parahaemoproteus*). Haemosporidian assemblages varied across elevations; each sampled range of elevations harbored abundant, yet host-specific lineages with different environmental associations. Bell's and Plumbeous Vireos, but not Gray Vireos, hosted several phylogenetically distinct, putative generalist lineages, likely reflecting spillover from more diverse local breeding bird communities. Repeated infections in individuals across breeding seasons, together with moderate parasitemia ($\bar{x} \approx 1\%$) suggest that these focal vireo species harbor chronic infections during their respective breeding seasons. These results demonstrate that elevational replacement patterns in avian hosts may be mirrored by their haemosporidian parasites, particularly among host-specialized lineages.
Keywords: Avian malaria, diversity, elevational range, haemosporidian, parasite, *Parahaemoproteus*, Vireonidae, *Vireo*, turnover

## 1. INTRODUCTION

Mountains harbor exceptional biodiversity, in part because elevational gradients tend to be finely partitioned by related species with ranges that are elevationally parapatric (Cadena and Loiselle, 2007; von Humboldt and Bonpland, 2009; Freeman et al., 2016). Yet, it remains unclear whether parasites of elevational replacement host species mirror this range stratification. Generally, host-parasite interactions can strongly influence biogeographic patterns, with reciprocal effects on fitness (Combes, 1997, 2001; Hasik and Siepielski, 2022; Poulin, 2011), population dynamics (Albon et al., 2002), and community structure (Minchella and Scott, 1991, McNew et al., 2021). Strong host-specificity, combined with shared environmental constraints, should result in parasite turnover that parallels the turnover of hosts along environmental gradients. Conversely, aspects of parasite life-history—such as insulation from climatic factors (e.g., endoparasites), dependency on secondary hosts and vectors (e.g., complex life cycle), and degree of host-specificity (e.g., host range and degree of host switching)—should be expected to cause discordant patterns from those observed in hosts (Gage et al. 2008; Krasnov and Poulin, 2010; Poulin and Krasnov, 2010; Ellis et al., 2015).

Regional surveys across elevational gradients reflect these complex relationships. In various mountain systems, parasite turnover has been found to exceed host turnover (Galen and Witt, 2014; Barrow et al., 2021), and host turnover has been found to predict parasite turnover (Ellis et al., 2015; Williamson et al., 2019; McNew et al., 2021). Gradients of precipitation and temperature, as well as landscape features, have also been found to shape parasite communities (Illera et al., 2017; McNew et al., 2021). Investigating the parasite communities of closely related host taxa that are elevational replacements provides a natural experiment for disentangling the relative roles of host associations, parasite traits, and environmental gradients in shaping parasite biogeography, while controlling for host

phylogeny, life history, and parasite susceptibility (Medeiros et al., 2013; Barrow et al., 2019).

Among blood parasites, haemosporidians (order Haemosporida; Danilewsky, 1885) are a cosmopolitan group of protozoans with complex life cycles dependent upon vertebrate taxa, including birds, mammals, and reptiles (Ricklefs and Fallon, 2002; Duval et al., 2007; Bensch et al., 2009; Galen et al., 2018; Boysen et al., 2022), and invertebrate vectors in the order Diptera (Linnaeus, 1758). A long history of co-evolution with avian hosts (Ricklefs and Fallon, 2002; Ricklefs et al., 2004; Lauron et al., 2015; Galen et al., 2018) has given rise to a remarkable diversity of avian haemosporidian lineages (Valkiūnas, 2005; Hellgren et al., 2007; Perkins, 2014), with many still yet to be described (Perkins, 2014; Borner et al., 2016; Galen et al., 2018). This diversity is reflected both phylogenetically and phenotypically, with variable degrees of pathogenicity (reviewed in Bennett et al., 1993) and host specificity (Ellis and Bensch, 2018; Fecchio et al., 2019) recorded among and within genera.

Given the high diversity and complexity of haemosporidian parasites, it has remained challenging to characterize the distribution patterns of haemosporidian lineages across large geographic scales (Clark, 2018). However, within regions and genera, spatial trends appear—reflecting the influence of climate directly, through physiological interactions during transmission and development (Ikemoto 2008; Mordecai et al., 2013), and indirectly, by influencing host and vector abundance and susceptibility (Filion et al., 2020). As a result, the fluctuating climate of temperate and montane regions produce seasonal, annual, and habitat-level waves of infection (Schrader et al., 2003; Bensch et al., 2007; Kim and Tsuda, 2010; Pérez-Rodríguez et al., 2013; Lutz et al., 2015; Reinoso-Pérez et al., 2024), whereas areas with higher, less seasonal temperatures, such as tropical regions and lowlands, can have persistent haemosporidian pressure (Zamora-Vilchis et al., 2012).

Infection intensity, commonly measured as parasitemia (defined as the 'estimated percentage of haemosporidians circulating in host blood') provides insight into host condition and stage of haemosporidian infection (i.e., acute or chronic; Valkiūnas, 2005). Like prevalence (here defined as 'proneness to infection'), parasitemia is also influenced by environmental factors, with peaks in temperate regions during the breeding season, when warmer, wetter conditions favor vector activity (Valkiūnas, 2005; Huang et al., 2020; Reinoso-Pérez et al., 2024) and when chronically infected hosts experience tissue-to-blood recrudescence (Atkinson and van Riper, 1991). Therefore, montane regions provide a valuable system for studying avian haemosporidian infection dynamics because of the sharp local variation in both climate and habitat over relatively small geographic distance (e.g., Illera et al., 2017; Rodríguez-Hernández et al., 2021; Williamson et al., 2019).

The southwestern U.S. presents a particularly compelling region for studying haemosporidian biogeography and dynamics due to its climatic heterogeneity, wide range of habitat types, and steep elevational gradients in sky island mountains. Although arid overall, the region exhibits strong variation in precipitation timing and intensity, shaped by both temperate seasonality and the North American monsoon system. These climatic patterns interact with topographic variation (reviewed in Coblentz and Riitters, 2004) to create a mosaic of ecologically distinct elevational zones ranging from lowland riparian corridors with high relative humidity and permanent water sources, to mid-elevation desert scrublands and savannas reliant on seasonal rainfall, to cooler montane forests with shorter growing seasons and higher annual precipitation (Sheppard et al., 2002). While community-level surveys suggest moderate overall prevalence of haemosporidian infection among avian communities in the region (mean: ~36%; Barrow et al., 2021), and while environmental conditions—particularly related to elevation, have been shown to strongly influence spatial patterns of infection (Williamson et al., 2019)—previous studies have primarily described

environmental and ecological contributions across mid-high elevation habitats and sky islands. Therefore, further work is needed to expand our understanding of whether observed environmental and elevational trends persist across broader gradients and habitat types, especially among particularly susceptible hosts.

Among the many avian species previously surveyed in the desert Southwest, the Plumbeous Vireo (*Vireo plumbeus*) has consistently stood out for its high haemosporidian prevalence across sites and years (Marroquin-Flores et al., 2017; Barrow et al., 2021). Migratory populations of this insectivorous songbird breed in mid- to high-elevation coniferous woodlands (from ~1,200–3,000 m) across the western U.S. and Mexico (Barlow, 1977; Curson and Goguen, 1998) and spend the nonbreeding season along the Pacific Slope and in the lowlands of central Mexico (Sibley and Monroe, 1990). Two closely related migratory vireos, Bell's Vireo (*Vireo bellii*) and Gray Vireo (*Vireo vicinior*), have relatively similar breeding distributions, yet inhabit distinct habitats and elevations. Gray Vireos breed in arid mid-elevation juniper (*Juniperus* spp.) savannas and chaparral, ~400–1,900 m (Hubbard, 1970; Barlow, 1977) and spend the nonbreeding season primarily in lowland desert and coastal areas of Sonora and Baja California (Barlow et al., 1999; Fischer et al., 2025). Bell's Vireos breed in lowland riparian habitats, generally below ~1,500 m, with comparatively high access to water and vegetative cover (Brown, 1993) and spend the nonbreeding season along the Pacific coast of Mexico, from Baja California and Sonora south to El Salvador. Given the similarities in ecology and life history among vireos, local differences in breeding elevational range make these three focal species an ideal comparative system through which to examine haemosporidian infection patterns across elevational gradients.

In this study, we tested whether haemosporidian biogeography, community assemblage, and infection dynamics vary predictably among three species of vireos that occupy distinct

143 elevations and habitats at sites in New Mexico and Utah, USA. Using a combination of
144 molecular screening and microscopy, we (1) compared parasite prevalence and infection
145 intensity among host species, including the first parasite survey for regionally vulnerable
146 Gray Vireos; (2) characterized haemosporidian haplotypes and host specificity; and (3) tested
147 the extent to which community composition was linked to elevational zones and/or their
148 associated host species and habitats. We predicted finding extensive parasite sharing between
149 elevational replacement vireo species, considering the proximity and interdigitated nature of
150 their ranges. Based on previously published haemosporidian surveys in vireos, we anticipated
151 finding high infection prevalence across all three host species; however, we also expected
152 prevalence and parasitemia to vary among species and environments. Lastly, because the
153 Southwest is arid, we predicted higher prevalence and parasite diversity in more mesic
154 habitats suitable for dipterid vectors, such as in the low-elevation riparian corridors used by
155 Bell's Vireos and high-elevation woodlands occupied by Plumbeous Vireos.
156

157 ## 2. MATERIALS AND METHODS

158 ### *2.1 Sample collection*

159 We sampled 248 wild-caught individuals of three vireo species (Bell's Vireo: $n = 20$,
160 Gray Vireo: $n = 170$, and Plumbeous Vireo: $n = 58$; Fig. 1A; Table S1). Sampled individuals
161 included adults and juveniles (Table S1). All individuals were sampled during the summer
162 months (May–August), with the majority sampled prior to monsoon season (~early-July–
163 September) from 1995–2019 across 28 unique sites in New Mexico and a single site in Utah.
164 During 2017–2019, targeted fieldwork was conducted to sample Gray Vireos: most
165 individuals were captured in mist nets, with the exception of hatch-year birds sampled at
166 nests. Blood samples were taken from the brachial vein and stored in lysis buffer, and
167 individuals were released at capture sites for ongoing study of Gray Vireo annual cycle

168 ecology (Fischer, 2020; Fischer et al., 2022; Fischer et al., 2025). In 2018 only, we prepared
169 and air-dried blood smears in the field ($n$ = 53). We also recaptured and collected a second
170 whole blood sample from fourteen Gray Vireos (approximately one year after their initial
171 sample collection in 2017), yielding two total whole blood samples and one smear for this
172 subset of individuals (Table S2). Additional Gray Vireo tissues for four individuals were
173 deposited at the Museum of Southwestern Biology (hereafter, MSB) at the University of New
174 Mexico following protocols approved by the UNM Institutional Animal Care and Use
175 Committee. Samples for Bell's and Plumbeous Vireos were requested as tissue loans from
176 the MSB. Detailed sampling protocol for Bell's and Plumbeous Vireos are described in
177 (Marroquin-Flores et al., 2017; Barrow et al., 2021; Gyllenhaal, 2024).
178 All sampled birds either had specific coordinates recorded at the time of capture or
179 were caught within 100 m of an existing sampling location. For the latter, we assigned
180 geographically proximate coordinates based on the nearest documented sampling site or,
181 when birds were captured between two closely spaced sites, by taking the midpoint between
182 them (Table S3).
183
184 ***2.2 Parasite screening and genetic data collection***
185 We extracted DNA from pectoral muscle ($n$ = 82) and whole blood ($n$ = 166) using
186 the QIAGEN DNeasy Blood and Tissue Kit following manufacturer's recommendations.
187 Birds were screened for *Haemoproteus* and *Plasmodium* parasites using three nested
188 polymerase chain reaction (PCR) protocols to amplify a 478-base pair (bp) fragment of the
189 haemosporidian mitochondrial cyt *b* gene (Hellgren et al., 2004; Waldenström et al., 2004).
190 We amplified parasite DNA with the outer primer pairs HaemNFI/HaemNR3 and
191 HaemNF/HaemNR2, followed by the nested primer pair HaemF/HaemR2. We prepared outer
192 PCR reactions in 25 µL volumes, containing 1.25 U of AmpliTaq Gold DNA Polymerase

193 (Applied Biosystems, Foster City, CA, USA), 1× PCR Buffer II, 2.5 mM MgCl2, 0.2 mM
194 dNTPs, 0.5 μM of each primer, and 20 ng of template DNA. Thermal cycling conditions
195 were modified from Galen and Witt (2014), with an initial denaturation at 95 °C for 8 mins,
196 followed by 20 cycles of 94 °C for 30 seconds, 50 °C for 30 secs, 72 °C for 45 secs, and a
197 final extension at 72 °C for 10 mins.
198 For nested PCR, we used 1 μL of the outer PCR product as the template, with reaction
199 conditions identical to the outer PCR, except for an increase to 35 cycles. Each reaction set
200 included negative and positive controls to monitor for contamination and confirm
201 amplification success, respectively. We visualized PCR products on 2% agarose gels stained
202 with SYBR Safe Gel Stain (Invitrogen, Carlsbad, CA, USA) to verify the presence of
203 amplicons of the expected size. Successfully amplified products were purified using ExoSap-
204 IT (Affymetrix, Inc., Santa Clara, CA, USA) and submitted for Sanger sequencing at
205 Psomagen (Rockville, MD, USA). Gray Vireo blood samples from recaptured individuals
206 (i.e., samples from the same individuals from 2017 and 2018) underwent PCR amplification,
207 but only a single sample was sequenced (Table S2).
208
209 ***2.3 Determining prevalence and haplotype diversity***
210 We determined positive infections upon successful amplification of haemosporidian
211 cyt *b* sequences and calculated pathogen prevalence within each host species by summing the
212 number of infected individuals for that species, divided by the total number of samples
213 screened for that species. Next, we calculated 95% binomial confidence intervals using the
214 'exact' method available in the *binom* package in R (version 4.3.2; R Core Team, 2023;
215 Sundar, 2006).
216 Haemosporidian cyt *b* forward and reverse reads were trimmed to remove primers,
217 resulting in the target fragment size of 478 bp and were then assembled using the default

218 alignment algorithm in Geneious (version 2025.03; Biomatters Ltd; Kearse et al., 2012; Table
219 S4). To identify haplotypes, we compared cleaned sequences to published records stored in
220 the public databases GenBank (National Center for Biotechnology Information, US National
221 Library of Medicine) and MalAvi (Bensch et al., 2009) by using the Basic Local Alignment
222 Search Tool (BLAST). Additionally, to ensure the accuracy of both established and novel
223 haplotypes, we downloaded all haemosporidian cyt *b* haplotype sequence files from MalAvi
224 and compared the number of differences, if any, to our sequences via a distance matrix
225 calculated in Geneious. Haplotypes that differed by one or more base pairs (~0.2% sequence
226 divergence) from published sequences on GenBank or MalAvi were considered novel and
227 named following MalAvi conventions. We compared coinfections with existing haplotypes in
228 our dataset to determine individual haplotypes when possible.
229
230 ***2.4 Phylogenetic analysis***
231 We estimated phylogenetic relationships among haemosporidian haplotypes using a
232 maximum-likelihood (ML) framework in RAxML, v8.2.10 (Stamatakis, 2014). Using the
233 GTR+G model of nucleotide substitution, we conducted a rapid bootstrap analysis with 1000
234 replicates, after which we searched for the best-scoring ML tree. We rooted the tree with
235 *Leucocytozoon* (COLBF21, GenBank Accession MK947795) based on the current
236 phylogenetic hypothesis for avian haemosporidians (Borner et al., 2016; Galen et al., 2018).
237 Nodes with <50% bootstrap support were collapsed in TreeGraph2 (Stöver and Müller,
238 2010). We determined the relationships among the three vireo study species based on the
239 posterior distribution of likely trees available on birdtree.org with the 'Hackett All Species'
240 option (Hackett et al., 2008; Jetz et al., 2012). We downloaded 100 phylogeny subsets and
241 selected the first tree because the relationships were consistent among the 100 trees.
242

243 ***2.5 Estimating parasite species richness and sampling completeness***

244 We used the *iNEXT* R package (version 3.0.1; Chao et al., 2014; Hsieh et al., 2024) to
245 estimate parasite lineage diversity and evaluate sampling completeness for host species with
246 adequate data (i.e., Gray and Plumbeous Vireos). In separate analyses for each host species,
247 we used infection counts of each parasite haplotype to generate rarefaction and extrapolation
248 curves for parasite species richness (q = 0), with the endpoint set at 400 individuals (i.e.,
249 infections). We applied the 'iNEXT()' function to compute species richness estimates,
250 including observed richness, extrapolated richness, and associated confidence intervals using
251 standard function parameters. Additionally, we used the output to estimate sampling
252 completeness (Chao et al., 2014) and defined this value as the minimum number of individual
253 birds required to detect 95% of the total estimated parasite haplotypes infecting each host
254 species. To visualize the rarefaction curves, we used the 'ggiNEXT()' function and *ggplot2*
255 package for style modifications (Wickham, 2016).

256

257 ***2.6 Microscopy and parasitemia calculations***

258 We obtained blood smears from the MSB for Plumbeous Vireos, when available (*n* =
259 28). Blood smears were made and air dried in the field for Gray Vireos (*n* = 53). We did not
260 obtain blood smears for Bell's Vireos. Each slide was fixed with absolute methanol and
261 stained for 50 mins with Giemsa solution (pH 7.0; Sigma-Aldrich, St. Louis, MO, USA). We
262 then examined each slide to confirm infection status using light microscopy on an Olympus
263 BX 53 Microscope following the protocol described in Valkiūnas (2005), where 10,000
264 erythrocytes were scanned at 1000x magnification with an oil immersion lens to identify and
265 count *Parahaemoproteus* and *Plasmodium* infections (Valkiūnas, 2005). We took digital
266 photographs of representative haemosporidian specimens, which were archived at the MSB
267 and are searchable via the Arctos database (https://arctos.database.museum/). If parasites

268 were found free-floating outside of erythrocytes, either due to the parasite's developmental
269 stage or by erythrocyte lysis due to factors during the preparation of the blood smear, they
270 were separately tallied and not included in the parasitemia calculation (Table S1). We
271 calculated parasitemia, or the estimated percentage of erythrocytes infected with
272 haemosporidian parasites, as the number of infected erythrocytes out of 10,000 screened. To
273 account for lack of normality in the data, we used a bootstrap method with 1,000 replications
274 to calculate parasitemia 95% confidence intervals via the R package *boot* (Kushary, 2000).
275
276 ***2.7 Characterizing environmental variation***
277 To obtain elevation in meters (m) from coordinates that did not contain original
278 elevation data, we used the 'elevation()' function from the R package *rgbif* (Chamberlain and
279 Boettiger, 2017; Chamberlain et al., 2024). We identified and removed elevation outliers
280 prior to analysis, as described in (Williamson and Witt, 2021).
281 We characterized climatic variation using 19 bioclimatic variables at 30 sec (~1 $km^2$)
282 resolution from the WorldClim 2.1 database (Fick and Hijmans, 2017). We used principal
283 components analysis (PCA) for temperature (Bio1–11) and precipitation (Bio12–19)
284 variables to create a composite measure of temperature and precipitation across the gradient.
285 The first two axes for temperature (hereafter, tempPC1 and tempPC2) explained a combined
286 84.2% of the variation and the first two axes for precipitation (hereafter, precipPC1 and
287 precipPC2) explained 95.1% of the variation (Fig. S1; Table S5-6). Variable loadings
288 indicated that tempPC1 primarily represented year-round temperatures, with higher values
289 relating to lower average temperatures, while tempPC2 represented greater seasonality and
290 less temperature stability, with higher values relating to more extreme temperature
291 fluctuations throughout the year and day-night cycle. Similarly, precipPC1 described the
292 overall precipitation amount, with higher values indicating wetter conditions, whereas

293 precipPC2 represented precipitation seasonality, with higher values representing more stable
294 and less seasonal precipitation (Table S5-6).
295
296 ***2.8 Assessing infection dynamics among host species and infection types***
297 We tested whether haemosporidian infection status differed between categorical
298 variables such as host species and tissue type (i.e., pectoral muscle or whole blood samples),
299 using Pearson's chi-squared tests via the *stats* package. To examine the relative magnitude of
300 effect for each comparison, we calculated Cramér's V effect sizes were using the 'CramerV()'
301 function in the *rcompanion* package (Mangiafico, 2024). Next, to assess differences in
302 parasitemia, we first normalized the data using a natural log ln(1+x) transformation and
303 removed two influential outliers with parasitemia >4% (Gray Vireo IDs: 272132427 and
304 272132642). We then evaluated residual variance with the 'var.test()' function in the *stats*
305 package and compared log-transformed parasitemia between Gray and Plumbeous Vireos and
306 infection types (i.e., single vs. coinfected) using two-tailed Student's *t*-tests.
307
308 ***2.9 Intraspecific infection prevalence and parasitemia across environments***
309 We employed a two-pronged approach to assess environmental associations with
310 infection prevalence: First, we used univariate, non-parametric tests to characterize and
311 compare intraspecific infection patterns across abiotic variables relevant to parasite and
312 vector ecology, including elevation, overall temperature (tempPC1) and precipitation
313 (precipPC1), and the seasonality of temperature (tempPC2) and precipitation (precipPC2).
314 Then, we built intraspecific multivariate linear models and applied nested and exhaustive
315 model selection to evaluate the strength and direction of environmental effects. We adopted
316 this approach to account for the structure of our data (i.e., non-overlapping elevational and

environmental bands distinctly correlated to species identity) and limitations of our dataset (i.e., limited sample sizes, degree of environmental variation, and infection class imbalances).

We first assessed data normality both visually, using the 'qqplot()' function from the *car* package (Fox and Weisberg, 2019), and then statistically, using the Shapiro-Wilk test using the 'shapiro.test()' function from the *stats* package. Given the non-normal distribution of environmental and geographic data in our dataset, we applied a rank-sum approach via Mann-Whitney U-tests to compare the distributions of environmental variables between infected and uninfected birds. Wilcoxon effect sizes of each comparison were then calculated via the 'wilcox_effsize()' function in the *rstatix* package (Kassambara, 2023).

We then constructed species-specific generalized linear models using glm() from the *stats* package. Prevalence model sets used a binomial distribution (hereafter: "BEVI_prev" for Bell's Vireo, "GRVI_prev" for Gray Vireo, and "PLVI_prev" for Plumbeous Vireo sets), while parasitemia model sets used a Gaussian distribution ("GRVI_para", "PLVI_para"). We evaluated linearity between the logit (log(probabilities/1-probabilities)) and predicted values in prevalence models visually via *ggplot2* package and assessed residual diagnostics in parasitemia models and with 'autoplot()' within the *ggfortify* package (Tang et al., 2016). Multicollinearity between variables was assessed by calculating variance inflation factors (VIF) via the *car* package. As expected, there was high collinearity with aspects of geographic and topographic variation, i.e. latitude and elevation, with other environmental variables. We retained elevation in all model sets because it captured variation in habitat and vector dynamics important to infection that were not explained by temperature and precipitation alone (Ishtiaq and Barve, 2018); however, we removed latitude from all linear models to reduce overfitting.

For model sets with adequate sampling (i.e., GRVI_prev, PLVI_prev, GRVI_para, PLVI_para), we evaluated all possible additive combinations of five predictor variables:

elevation, tempPC1, tempPC2, precipPC1, precipPC2. We used the 'dredge' function in the *MuMIn* package (Bartoń, 2024) for exhaustive model selection. For host datasets with < 30 data points (BEVI_prev and PLVI_para) we restricted candidate models to simple, biologically relevant structures to avoid overfitting. Specifically, we included univariate models nested within simple additive models containing at most two predictor variables, as well as null and global models for comparison. We then compared model performance and evaluated the trade-off between model fit and complexity using Akaike's Information Criterion corrected for small sample sizes (AICc; Table 1).

To examine the effect of each predictor in top-ranked models, we standardized and calculated model-averaged regression coefficients using the *MuMIN* package (Table 2). For top-ranked models where the null model was not favored, we assessed goodness of fit via Hosmer-Lemeshow tests as part of the *ResourceSelection* package (Lele et al., 2023) and checked for overdispersion by dividing residual deviance by the degrees of freedom. Predictive accuracy was also assessed using 10-fold cross-validation via the *caret* package (Kuhn, 2008).

## 3. RESULTS

### *3.1 Haemosporidian prevalence, abundance, and diversity*

We uncovered an unusually high prevalence of haemosporidian infections in all three vireo species, with 175 infected birds of 248 screened (70.6%; 95% CI [64.5 – 76.2%]). The highest documented prevalence was found in Plumbeous Vireos (84.5% infected; 95% CI [72.6 – 92.7%]), followed by Gray Vireos (67.7%; 95% CI [60.0 – 74.7%]), and lastly, Bell's Vireos (55%; 95% CI [31.5 – 76.9%]; Fig. 1B). Prevalence was significantly lower in Bell's than in Plumbeous Vireos ($\chi^2(1) = 5.72$, $p = 0.017$, $\varphi = 0.31$), indicating a moderate effect size. While most birds were infected by single haemosporidian haplotype infections (88.1%;

367 95% CI [82.3 – 92.5%]), we found 21 individuals that were coinfected with two or more
368 haplotypes (12.0%; 95% CI [7.54 – 17.7%]), and one Gray Vireo that was infected by three
369 haplotypes (VIRVIC01, VIRVIC02, VIRVIC03). Of the 14 Gray Vireos recaptured about a
370 year after initial sampling, 12 were infected with haemosporidians in both years, while two
371 that were uninfected in 2017 tested positive in 2018.

372 Nearly all infections were caused by parasites in the genus *Haemoproteus*,
373 specifically the subgenus *Parahaemoproteus* (99.5%), which comprised 18 of 19 haplotypes
374 identified. *Plasmodium* was rare in our data, with a single infection (lineage VIRPLU13)
375 recorded from a Plumbeous Vireo (MSB:Bird:60726; Table S4). Of the 19 total parasite
376 haplotypes identified, 8 were novel (Fig. 1D; Table S4).

377

378 ***3.2 Estimates of parasite species richness and sampling completeness***

379 We identified a total of three haemosporidian haplotypes from Bell's Vireos, four
380 from Gray Vireos, and 14 from Plumbeous Vireos (Fig. 1D). These differences were partly,
381 but not entirely, attributable to differences in sample size. Gray Vireo *Parahaemoproteus*
382 infections were substantially less diverse than those of Plumbeous Vireos despite more
383 intensive screening efforts. Extrapolation from rarefaction curves showed considerably lower
384 estimated parasite richness for Gray Vireos (4.99 ± 0.53 SE; 95% CI [4.00–6.03]; Table S7)
385 and estimated that much smaller sample sizes would be needed to reach 95% sampling
386 completeness (14 infections; Fig. 2; Table S8). This result contrasted our results for
387 Plumbeous Vireos, where parasite richness was estimated to be ~10x higher than Gray Vireos
388 (53.8 ± 23.3 SE; 95% CI [14.0–99.6]) and require much greater sampling effort (~26x more
389 than estimated for Gray Vireos) to reach an estimated 95% completeness (estimated 364
390 infections). Bell's Vireos also exhibited low lineage diversity (3.92 ± 0.784 SE; 95% CI
391 [3.00-5.45] and an estimated 95% sample completeness at only 33 infections, consistent with

392 the limited diversity recovered (Table S7-S8). However, we caution overinterpreting these
393 results due to the small Bell's Vireo sample size (*n* = 12 infected) in our study and
394 recommend additional sampling to generate more precise estimates.
395 Of the 19 total haplotypes identified, we found evidence of potential host specificity
396 with at least one species-specific haplotype infecting each of the three vireo species (Table
397 S4). Of note, Gray Vireos were infected by novel haemosporidian haplotypes only,
398 (VIRVIC01-VIRVIC04). This finding contrasted with Plumbeous Vireos, which showed
399 novel haplotypes (i.e. VIRPLU10-13) and haplotypes previously found only in Plumbeous
400 Vireos (i.e. VIRPLU03, VIRPLU07-09), as well as lineages known to infect other non-vireo
401 species (i.e. SETAUD14, TROAED12, VIGIL07, VIRPLU01, and VIRPLU04). Sampling
402 was comparatively lower for Bell's Vireos; no novel lineages were detected. We did detect,
403 however, a recently described lineage (VIRBEL01) which was previously documented in
404 Bell's Vireos sampled from Arizona and Texas (Fecchio et al., 2023), as well as other more
405 generalist lineages (i.e. TROAED12 and VIGIL07; Table S4).
406
407 ***3.3 Intensity of infection (parasitemia) across hosts and haplotypes***
408 We screened 102 individuals via microscopy (Gray *n* = 71, Plumbeous *n* = 31). A
409 total of 81 samples showed evidence of infection and had parasitemia *calculated*
410 *(Parahaemoproteus:* Gray *n* = 53 and Plumbeous *n* = 27; *Plasmodium*: Plumbeous *n* = 1).
411 Gray Vireos typically had slightly higher infection loads (1.00%; 95% CI [0.782 – 1.27%])
412 compared to Plumbeous Vireos (0.786%; 95% CI [0.584 – 1.01%]), partly due to two outlier
413 Gray Vireo samples with >4% parasitemia (ID 272132427 and 27213264; Fig 1C). After
414 removing these outliers, we found that mean parasitemia did not differ significantly between
415 host species (t(77) = 0.656, p = 0.514). When we compared single-haplotypes and
416 coinfections, we also found no significant difference in parasitemia between species (t(73) = -

417 0.728, p = 0.469), though we note the sampling pool of coinfected birds was small compared
418 to single infections ($n$ = 7 and $n$ = 68, respectively).
419 Our comparison of infections using PCR and microscopy was largely consistent, with
420 few detection errors identified between the two methods. We detected four positively infected
421 birds via microscopy that did not successfully amplify by PCR (Table S1). These samples
422 had a range of parasitemia spanning 0.70% to 2.68%. Additionally, we failed to detect
423 haemosporidian infections via microscopy for two birds that were later successfully amplified
424 using PCR; one individual was the single coinfected Gray Vireo with three
425 *Parahaemoproteous* haplotypes that were identified by sequencing (Table S1).
426
427 ***3.4 Environmental patterns of infection status and parasitemia***
428 *Parahaemoproteus* prevalence showed idiosyncratic patterns among host species and
429 their associated habitats (Fig 3; Table S9). For example, we found that infected Bell's Vireos
430 tended to be found at lower latitudes ($z$ = -2.09, $p$ = 0.040), with warmer year-round
431 temperatures (tempPC1; $z$ = -2.25, $p$ = 0.027 Fig. 3; Fig. S2; Table S9). Similarly, probability
432 of infection increased as overall precipitation (precipPC1) and temperature seasonality
433 (tempPC2) increased (Table 1; Table 2). In contrast, we found higher proportions of infected
434 Gray Vireos at lower elevations ($z$ = -2.07, $p$ = 0.038), Fig. 1C; Table S9) and at sites with
435 more stable precipitation (precipPC2; z = 1.72, p = 0.057), Fig 3; Table S9). However, this
436 result was dampened when we excluded the eleven infected Gray Vireos from the Abajo
437 Mountain site in Utah, which were outliers in many of the environmental PCA dimensions.
438 The top model, however, showed that infection was negatively associated with elevation and
439 positively associated with temperature (tempPC1; Table 1; Table 2) even when excluding the
440 Utah site. Lastly, Plumbeous Vireo infections tended to be higher in areas with more
441 seasonally stable precipitation (precipPC2; $z$ = 2.04, $p$ = 0.042), Fig. 3). Despite the top-

442 ranked infection probability model showing no significant linear trends, precipitation
443 (precipPC1 and precipPC2) was present in the majority of top candidate models (Table 1).
444 We did not find any association between parasitemia and environmental variables in
445 Plumbeous Vireos, with the null model having the strongest support and no clear predictor
446 variable significantly reported across top models (Table S10). Gray Vireos, however, showed
447 a significant pattern of increased parasitemia as overall precipitation (precipPC1) increased
448 (Table S10), but this model had low explanatory power ($R^2 = 0.05$).
449
450 4. DISCUSSION
451 Vireo species breeding in the southwestern U.S. are especially susceptible to
452 haemosporidian infection, particularly by parasites in the *Parahaemoproteus* subgenus. In
453 this study, we uncovered that the elevational limits of haemosporidian parasites closely
454 parallel those of their avian hosts. We observed striking differences in host specificity and
455 parasite richness across host species and their associated habitats, revealing that the high-
456 elevation Plumbeous Vireos harbored the most diverse and phylogenetically distinct parasite
457 lineages, especially compared to another well-sampled, lower elevation host species, the
458 Gray Vireo. Although parasite prevalence differed significantly between Bell's Vireos (55%
459 infected) and Plumbeous Vireos (86.2% infected), which breed under different levels of
460 precipitation and temperature, we found variable links between infection status and climatic
461 factors in our dataset. Specifically, we found that infection probability was strongly
462 influenced by aspects of temperature for Bell's Vireos, elevation for Gray Vireos, and
463 precipitation for Plumbeous Vireos, likely reflecting subtle differences in habitat suitability
464 for arthropod vectors. Lastly, we found low to moderate parasitemia values in both Gray and
465 Plumbeous Vireos, consistent with chronic infections. We examine these results in relation to

466 previous haemosporidian research in the southwest U.S. and in vireos, both in their breeding
467 and nonbreeding grounds, and discuss remaining questions in the sections below.
468
469 ***4.1 Elevational replacement and haemosporidian diversity patterns***
470 Avian haemosporidians exhibit variable patterns of turnover across elevations (Galen
471 and Witt, 2014; Illera et al., 2015; McNew et al., 2021), which is often independent of
472 geographic distance between hosts (Williamson et al., 2019; Barrow et al., 2021). We
473 demonstrated a strong case of parallel elevational replacement in hosts and parasites, with
474 high turnover among *Parahaemoproteus* assemblages infecting vireo species breeding at
475 different elevations. This elevational replacement pattern could be the result of a few
476 different scenarios. For example, shared historical and ecological forces, such as habitat
477 specialization in both hosts and vectors (Ellis et al., 2020), may shape the elevational range
478 limits of both vireos and their *Parahaemoproteus* parasites. Alternatively, species-specific
479 factors that co-evolved independently in response to specialized parasite lineage pressures,
480 such as immune defenses (e.g., Armour et al., 2025), could also be at play. Whether parasite
481 elevational replacement is host-driven or independently mediated by the environmental
482 gradient, global patterns of spatial diversity in parasites should be tightly coupled with those
483 of their hosts.
484 Of the 30 cyt *b Parahaemoproteus* and 12 *Plasmodium* haplotypes currently reported
485 to infect vireo species (MalAvi; downloaded 1/1/2025), our study adds seven novel
486 *Parahaemoproteus* and one novel *Plasmodium* haplotype. The near absence of *Plasmodium*
487 infections, even at lower elevations, contrasts findings from other temperate region studies
488 (e.g. in Alaska: Oakgrove et al., 2014; California: Walther et al., 2016; Oklahoma: Wyckoff
489 et al., 2024) but is consistent with previous screening at high elevations in New Mexico
490 (Marroquin-Flores et al., 2017; Williamson et al., 2019; Barrow et al., 2021). While the

491 cooler temperatures experienced at higher elevations have been proposed as a potential
492 limiting factor for haemosporidian infection (e.g. LaPointe et al., 2012; Barrow et al., 2021),
493 the low prevalence of *Plasmodium* at lower elevations in this region may also reflect limited
494 suitable habitat for mosquito vectors prior to the onset of monsoon rains. Broader and
495 temporally replicated surveys of potential vectors and vector abundance in this region are
496 needed to fully explain this apparent absence.

497 We identified an interesting pattern among the *Parahaemoproteus* lineages found in
498 our focal species: Plumbeous Vireos harbored a broad diversity of parasite haplotypes
499 relative to the other two sampled species, while Gray Vireos exhibited a depauperate and
500 likely specialized haemosporidian assemblage (Fig. 1D). This disparity suggests that
501 Plumbeous Vireos may support more permissive or ecologically flexible parasite
502 associations, while Gray Vireos may be undergoing, or may have already undergone, a
503 transition toward fixed symbiosis with a narrower set of haemosporidian lineages. Although
504 the degree of cyt *b* divergence among lineages is generally low (<5% in most haplotypes
505 based on post-hoc Jukes–Cantor distance assessments), a few lineages (e.g., SETAUD14,
506 VIRPLU07) diverge more substantially (>5%) from others such as VIRVIC01–03 and
507 TROAED12 (Hellgren et al., 2007; Table S11). The contrasting pattern of haemosporidian
508 diversity between vireo species could alternatively be caused by differences in avian host
509 richness, and the low diversity found in Gray Vireos could reflect the depauperate breeding
510 bird communities of the arid and structurally simple juniper savanna habitats.

511

512 ***4.2 Conserved high susceptibility to haemosporidians among vireo species***

513 Vireos stand out among southwestern songbirds for their consistently high
514 haemosporidian infection rates, providing a valuable opportunity to examine parasite
515 dynamics in hyper-susceptible hosts. In the three species screened here, we found that 70.6%

516 of 248 individuals screened had at least one haemosporidian infection, which is greater than
517 double the prevalence reported in broader community-wide surveys conducted in the
518 southwestern U.S. over a similar period. For example, Marroquin-Flores et al. (2017)
519 screened 186 birds of 49 species sampled in New Mexico from June-July 2016, including 13
520 individual vireos of two species: *n* = 4 Warbling Vireos (*Vireo gilvus*) and *n* = 9 Plumbeous
521 Vireos. The average proportion of infection was 36.6% across all studied species, but 92% of
522 vireos tested positive. A subsequent large-scale study by Barrow et al. (2021) reported similar
523 patterns, with an overall haemosporidian prevalence of 36.1% among 776 total individuals of
524 61 species. Of these, vireos again exhibited significantly higher infection proportions, with
525 Plumbeous and Warbling Vireos demonstrating the highest prevalence in the study at 87%
526 and 78%, respectively (Barrow et al., 2021).

527 This observation of high susceptibility in vireos is not limited to birds sampled in the
528 southwestern U.S., as other studies across breeding sites have also reported higher relative
529 prevalences in the *Vireo* genus. Granthon and Williams (2017) reported that 100% of the 62
530 PCR-screened Red-eyed Vireos (*Vireo olivaceus*) from Pennsylvania were infected with
531 *Plasmodium*, *Haemoproteus*, or *Leucocytozoon* species (Granthon and Williams, 2017).
532 Rodriquez et al. (2021) found *Haemoproteus* prevalence of 59% in 22 individual Warbling
533 Vireos sampled from Colorado breeding sites (Rodriguez et al., 2021). Shared susceptibility
534 within closely related species has been extensively documented (e.g. González et al., 2014;
535 Lutz et al., 2015; Barrow et al., 2019; Pigeault et al., 2022) but attempts to identify the
536 specific factors that contribute to high prevalence in vireos are still lacking. Of the conserved
537 host traits recorded to have consistent interaction with haemosporidian prevalence in other
538 avian clades, thus far, shared life history traits such as open cup nest type and insectivorous
539 diets (as reported and reviewed in Braga et al., 2011; Rodriguez et al., 2021) may increase
540 exposure risk, at least partially explaining the high prevalence in this group. However, a

541 combination of traits, including behavior (e.g., time spent incubating and/or brooding at the
542 nest), features of nest microhabitat (e.g., height of nest from ground), and aspects of
543 immunity (e.g., haemosporidian tolerance) may also contribute to the elevated susceptibility
544 (González et al., 2014; Lutz et al., 2015; Muriel, 2020; Rodriguez et al., 2021; Pigeault et al.,
545 2022).

546 Interestingly, of the 14 Gray Vireos that we recaptured and screened for parasites
547 across two sampling years (2017 and 2018), 12 were positive via PCR in both years, and the
548 remaining two birds became infected by the second year (Table S2). Although more data is
549 needed to determine whether these represent chronic infections or reinfections, and pinpoint
550 where transmission occurs, these results indicate Gray Vireos likely experience sustained
551 parasite pressure during the breeding season. Continued monitoring of haemosporidian
552 infection across vireo populations, coupled with investigations into the mechanisms
553 underlying their susceptibility, could yield valuable insights into the spatial and temporal
554 dynamics of infection risk in this clade.

555

556 ***4.3 Environmental determinants of haemosporidian infection vary by host species***

557 Previous studies have found strong links between haemosporidian prevalence and
558 topographic, geographic, and climatic variables (Pérez-Rodríguez et al., 2013; Rodriguez et
559 al., 2021), but the direction and magnitude of these effects vary by region and
560 haemosporidian clade (Williamson et al., 2019). In the arid southwest, we expected
561 haemosporidian prevalence to correspond with water availability, which is important for
562 insect vector (Valkiūnas, 2004; Santiago-Alarcon et al., 2012), such as those associated with
563 potential water sources (i.e. riparian habitats) and areas with higher, more seasonally stable
564 precipitation (i.e. montane woodlands). Somewhat contrary to expectations given predictions
565 about the relative aridity of habitat during the pre-monsoon sampling period, we found that

566 interspecific differences in prevalence increased linearly with elevation and precipitation:
567 Bell's Vireos showed the lowest prevalence and Gray Vireos exhibited unexpectedly high
568 infection rates. We were unable to determine whether observed infection patterns were driven
569 by species-specific traits or abiotic environmental differences, and increased sampling of
570 Bell's Vireos may help clarify or reduce these differences. Within-species analyses revealed
571 no consistent predictors of infection across all taxa (Fig. S2-6); instead, different
572 environmental variables were associated with infection in each species (Fig. 3; Table S9-
573 S10). Expanded screening of haemosporidians across low- to mid-elevation habitats, among
574 co-distributed species, at variable distance from water sources, and across precipitation
575 gradients would further elucidate cross-elevational trends and enhance predictions of
576 infection probability in avian communities of the southwestern U.S.
577
578 ***4.4 Moderate and consistent infection loads across environmental gradients***
579 Gray and Plumbeous Vireos exhibited similar average infection loads (~1% in Gray
580 Vireos, 0.786% in Plumbeous, range: 0.03–4.5%) with no significant differences between
581 species (Fig. 1B). These values slightly exceed the regional cross-species average (<1%;
582 Marroquin-Flores et al., 2017) and fall within the range of moderate infection intensities
583 reported in experimental studies of other passerines (e.g. Asghar et al., 2012). We did note,
584 however, two Gray Vireos with elevated parasitemia (4.5 and 4.49%) were sampled at
585 distinct sites in the Sevilleta National Wildlife Refuge. The elevated parasitemia in these
586 individuals likely represented acute infection acquired shortly before capture and prior to
587 immune response, or recrudescence of chronic infections exacerbated by physiological
588 stressors such as nutritional deficits or hormonal fluctuations (Arriero et al., 2018; Names et
589 al., 2021). The absence of high parasitemia in Bell's and Plumbeous Vireos could be an
590 artifact of limited sampling, as birds with severe infections often exhibit reduced mobility

591 and capture probability (Mukhin et al., 2016), suggesting that heavily infected individuals in
592 these species may be underrepresented.
593 Additionally, we found no relationship between parasitemia and any tested
594 environmental variables for Plumbeous Vireos. In Gray Vireos we saw a significant linear
595 trend in parasitemia with increased overall precipitation (precipPC1; Table S10), but this
596 model had weak explanatory power ($R^2 = 0.05$). These results are consistent with previous
597 findings which suggest that haemosporidian parasitemia patterns are shaped by complex
598 interactions between host and parasite biology not easily captured in models with abiotic
599 factors alone (Loiseau et al., 2013).
600
601 ***4.5 Remaining questions***
602 First, expanding screening to include *Leucocytozoon* parasites of vireos would
603 provide a useful contrast with *Parahaemoproteus*; this could be especially important at high
604 elevations, since *Leucocytozoon* is more common at cooler, high-elevation sites and has been
605 detected in Plumbeous Vireos in this region (Galen and Witt, 2014; Marroquin-Flores et al.,
606 2017; Barrow et al., 2019; Barrow et al., 2021). Second, incorporating a multi-locus nuclear
607 DNA data (as described in Barrow et al., 2018), together with morphological data, could
608 provide greater resolution for distinguishing closely related *Parahaemoproteus* haplotypes,
609 offering clearer insights into their evolutionary history and host specificity. Finally, the host
610 species-specific environmental patterns that we captured might reflect dynamics of arthropod
611 vectors, which still remain largely uncharacterized in the southwestern United States.
612
613 ***4.6 Conclusions***
614 In this study, we found that parasite elevational distributions mirror the elevational
615 replacement pattern of host species among vireos in southwestern North America.This

616 pattern may have resulted from host specialization, climate variation independently acting on
617 hosts and parasites, climate variation acting indirectly through habitat or broader host and
618 vector communities, or a combination of those forces. We found that vireos were consistently
619 infected at high rates and largely harbor chronic, low-to-moderate intensity infections
620 dominated by *Parahaemoproteus*, suggesting the potential for exclusive, reciprocal selective
621 pressures that facilitate host-parasite coadaptation. The contrast in parasite richness between
622 Plumbeous Vireos and Gray Vireos was striking: Gray Vireos harbored a limited number of
623 haemosporidian lineages, all of which were host specific, while Plumbeous Vireos were
624 infected with a diverse set of lineages. These differences imply species-specific variability in
625 resistance, tolerance, or exposure to generalist haemosporidian lineages. In sum, our work
626 adds to a growing body of evidence about clade-specific avian host susceptibility and host-
627 parasite turnover across elevational gradients, highlighting vireos as an ideal focal group for
628 future work on host-parasite dynamics across space and time.

ACKNOWLEDGEMENTS

The authors sincerely thank Bethany Abrahamson, Michael Andersen, Matthew Baumann, Alison Boyer, Serina Brady, Sara Brant, Mariel Campbell, Andrea Chavez, Mina Carnicom, Lida Crooks, Rosario Marroquin-Flores, Chauncey Gadek, Spencer Galen, Ethan Gyllenhaal, Mike Hartshorne, Andy Johnson, Tae Kunisawa, Michael Lelevier, Joseph Manthey, Xena Mapel, Taylor Martinez, Jenna McCullough, Moses Michelsohn, Kathleen Ramsay, George Rosenberg, C. Jonathan Schmitt, Donna Schmitt, Brenda Villanueva, and Toby Weisenhaus for their support and contributions.

637 REFERENCES

638 Albon, S.D., Stien, A., Irvine, R.J., Langvatn, R., Ropstad, E., Halvorsen, O., 2002. The role of
639 parasites in the dynamics of a reindeer population. Proc. R. Soc. Lond. B Biol. Sci. 269,
640 1625–1632. https://doi.org/10.1098/rspb.2002.2064.

641 Arriero, E., Pérez-Tris, J., Ramírez, A., Remacha, C., 2018. Trade-off between tolerance and
642 resistance to infections: an experimental approach with malaria parasites in a passerine bird.
643 Oecologia 188, 1001–1010. https://doi.org/10.1007/s00442-018-4290-4.

644 Armour, C., Hone A.L., Dunn J.C., 2025. Do specialist haemoparasites induce tolerance in their
645 hosts? Parasitology. 152, 374–380. https://doi.org/10.1017/ S0031182025000393.

646 Asghar, M., Westerdahl, H., Zehtindjiev, P., Ilieva, M., Hasselquist, D., Bensch, S., 2012. Primary
647 peak and chronic malaria infection levels are correlated in experimentally infected great
648 reed warblers. Parasitology 139, 1246–1252. https://doi.org/10.1017/S0031182012000510.

649 Atkinson, C.T., van Riper, C., 1991. Pathogenicity and epizootiology of avian haematozoa:
650 *Plasmodium, Leucocytozoon, and Haemoproteus*, in: Loye, J.E., Zuk, M. (Eds.), Bird-
651 Parasite Interactions: Ecology, Evolution, and Behavior. Oxford Academic Press, pp. 19–48.

652 Barlow, J.C., 1977. Effects of habitat attrition on vireo distribution and population density in the
653 northern Chihuahuan Desert, in: Wauer, R.H., Riskind, D.H. (Eds.), Transactions of the
654 Symposium on the Biological Resources of the Chihuahuan Desert Region, United States
655 and Mexico. U.S. Department of the Interior National Park Service Trans. Proc., pp. 591–
656 596.

657 Barlow, J.C., Leckie, S.N., Baril, C.T., 1999. Gray Vireo (*Vireo vicinior*), in: Poole, A., Gill, F.
658 (Eds.), The birds of North America. The Academy of Natural Sciences, Philadelphia, PA,
659 and The American Ornithologists' Union, Washington, D.C.

660 Barrow, L.N., Bauernfeind, S.M., Cruz, P.A., Williamson, J.L., Wiley, D.L.F., Ford, J.E.,
661 Baumann, M.J., Brady, S.S., Chavez, A.N., Gadek, C.R., Galen, S.C., Johnson, A.B.,
662 Mapel, X.M., Marroquin-Flores, R.A., Martinez, T.E., McCullough, J.M., McLaughlin, J.E.,

Witt, C.C., 2021. Detecting turnover among complex communities using null models: a case study with sky-island haemosporidian parasites. Oecologia 195, 435–451. https://doi.org/10.1007/s00442-021-04854-6.

Barrow, L.N., Lemmon, A.R., Lemmon, E.M., 2018. Targeted sampling and target capture: assessing phylogeographic concordance with genome-wide data. Syst. Biol. 67, 979–996. https://doi.org/10.1093/sysbio/syy021

Barrow, L.N., McNew, S.M., Mitchell, N., Galen, S.C., Lutz, H.L., Skeen, H., Valqui, T., Weckstein, J.D., Witt, C.C., 2019. Deeply conserved susceptibility in a multi-host, multi-parasite system. Ecol. Lett. 22, 987–998. https://doi.org/10.1111/ele.13263.

Bartoń, K. 2024. MuMIN: Multi-model inference. R package version 1.48.4. https://CRAN.R-project.org/package=MuMIn.

Bennett, G.F., Peirce, M.A., Ashford, R.W., 1993. Avian Haematozoa: mortality and pathogenicity. J. Nat. Hist. 27, 993–1001. https://doi.org/10.1080/00222939300770621.

Bensch, S., Hellgren, O., Pérez-Tris, J., 2009. MalAvi: a public database of malaria parasites and related haemosporidians in avian hosts based on mitochondrial cytochrome *b* lineages. Mol. Ecol. Resour. 9, 1353–1358. https://doi.org/10.1111/j.1755-0998.2009.02692.x.

Bensch, S., Waldenström, J., Jonzén, N., Westerdahl, H., Hansson, B., Sejberg, D., Hasselquist, D., 2007. Temporal dynamics and diversity of avian malaria parasites in a single host species. J. Anim. Ecol. 76, 112–122. https://doi.org/10.1111/j.1365-2656.2006.01176.x.

Billerman, S. M., B. K. Keeney, G. M. Kirwan, F. Medrano, N. D. Sly, and M. G. Smith, Ed. 2025. Birds of the World. Cornell Laboratory of Ornithology, Ithaca, NY, USA. https://birdsoftheworld.org/bow/home.

Borner, J., Pick, C., Thiede, J., Kolawole, O.M., Kingsley, M.T., Schulze, J., Cottontail, V.M., Wellinghausen, N., Schmidt-Chanasit, J., Bruchhaus, I., Burmester, T., 2016. Phylogeny of haemosporidian blood parasites revealed by a multi-gene approach. Mol. Phylogenet. Evol. 94, 221–231. https://doi.org/10.1016/j.ympev.2015.09.003.

Boysen, K.E., Perkins, S.L., Hunjan, S., Oliver, P., Gardner, M.G., Balasubramaniam, S., Melville, J., 2022. Diversity and phylogenetic relationships of haemosporidian and hemogregarine parasites in Australian lizards. Mol. Phylogenet. Evol. 167, 107358. https://doi.org/10.1016/j.ympev.2021.107358.

Braga, É.M., Silveira, P., Belo, N.O., Valkiūnas, G., 2011. Recent advances in the study of avian malaria: an overview with an emphasis on the distribution of Plasmodium spp in Brazil. Mem. Inst. Oswaldo Cruz 106, 3–11. https://doi.org/10.1590/S0074-02762011000900002.

Brown, B.T., 1993. Bell's Vireo (*Vireo bellii*), in: Poole, A., Gill, F. (Eds.), The birds of North America. The Academy of Natural Sciences, Philadelphia, PA, and The American Ornithologists' Union, Washington, D.C.

Cadena C.D., Loiselle B.A., 2007. Limits to elevational distributions in two species of emberizine finches: disentangling the role of interspecific competition, autoecology, and geographic variation in the environment. Eco. 30, 491–504

Chamberlain, S., Barve, V., Mcglinn, D., Oldoni, D., Desmet, P., Geffert, L., Ram, K., 2024. rgbif: Interface to the global biodiversity information facility API.

Chamberlain, S.A., Boettiger, C., 2017. R Python, and Ruby clients for GBIF species occurrence data. https://doi.org/10.7287/peerj.preprints.3304v1.

Chao, A., Gotelli, N.J., Hsieh, T.C., Sander, E.L., Ma, K.H., Colwell, R.K., Ellison, A.M., 2014. Rarefaction and extrapolation with Hill numbers: a framework for sampling and estimation in species diversity studies. Ecol. Monogr. 84, 45–67. https://doi.org/10.1890/13-0133.1.

Cicero, C., Koo, M.S., Braker, E., Abbott, J., Bloom, D., Campbell, M., Cook, J.A., Demboski, J.R., Doll, A.C., Frederick, L.M., Linn, A.J., Mayfield-Meyer, T.J., McDonald, D.L., Nachman, M.W., Olson, L.E., Roberts, D., Sikes, D.S., Witt, C.C., Wommack, E.A., 2024. Arctos: Community-driven innovations for managing natural and cultural history collections. PLOS ONE 19, e0296478. https://doi.org/10.1371/journal.pone.0296478.

714 Clark N.J., 2018. Phylogenetic uniqueness, not latitude, explains the diversity of avian blood
715 parasite communities worldwide. Glob Ecol Biogeogr 27, 744–755.
716 https://doi.org/10.1111/geb.12741.
717 Coblentz, D.D., Riitters, K.H., 2004. Topographic controls on the regional-scale biodiversity of the
718 south-western USA. J. Biogeogr. 31, 1125–1138. https://doi.org/10.1111/j.1365-
719 2699.2004.00981.x.
720 Combes, C., 2001. Parasitism: the ecology and evolution of intimate interactions. University of
721 Chicago Press, Chicago and London.
722 Combes, C., 1997. Fitness of parasites: Pathology and selection. Int. J. Parasitol. 27, 1–10.
723 https://doi.org/10.1016/S0020-7519(96)00168-3.
724 Curson, D.R., Goguen, C.B., 1998. Plumbeous Vireo (*Vireo plumbeus*), in: Poole, A., Gill, F.
725 (Eds.), The birds of North America, Inc., Philadelphia, PA.
726 Duval, L., Robert, V., Csorba, G., Hassanin, A., Randrianarivelojosia, M., Walston, J., Nhim, T.,
727 Goodman, S.M., Ariey, F., 2007. Multiple host-switching of Haemosporidia parasites in
728 bats. Malar. J. 6, 157. https://doi.org/10.1186/1475-2875-6-157.
729 Ellis, V.A., Bensch, S., 2018. Host specificity of avian haemosporidian parasites is unrelated among
730 sister lineages but shows phylogenetic signal across larger clades. Int. J. Parasitol. 48, 897–
731 902. https://doi.org/10.1016/j.ijpara.2018.05.005.
732 Ellis, V. A., Collins, M. D., Medeiros, M. C. I., Sari, E. H. R., Coffey, E. D., Dickerson, R. C.,
733 Lugarini, C., Stratford, J. A., Henry, D. R., Merrill, L., Matthews, A. E., Hanson, A. A.,
734 Roberts, J. R., Joyce, M., Kunkel, M. R., Ricklefs, R. E., 2015. Local host specialization,
735 host-switching, and dispersal shape the regional distributions of avian haemosporidian
736 parasites. Proc. Natl. Acad. Sci. 112(36), 11294–11299.
737 https://doi.org/10.1073/pnas.1515309112.
738 Ellis, V. A., Huang, X., Westerdahl, H., Jönsson, J., Hasselquist, D., Neto, J. M., Nilsson, J.,
739 Nilsson, J., Hegemann, A., Hellgren, O., Bensch, S., 2020. Explaining prevalence, diversity

and host specificity in a community of avian haemosporidian parasites. Oikos 129(9), 1314–1329. https://doi.org/10.1111/oik.07280.

Fecchio, A., Bell, J.A., Williams, E.J., Dispoto, J.H., Weckstein, J.D., De Angeli Dutra, D., 2023. Co-infection with *Leucocytozoon* and other haemosporidian parasites increases with latitude and altitude in New World bird communities. Microb. Ecol. 86, 2838–2846. https://doi.org/10.1007/s00248-023-02283-x.

Fecchio, A., Wells, K., Bell, J.A., Tkach, V.V., Lutz, H.L., Weckstein, J.D., Clegg, S.M., Clark, N.J., 2019. Climate variation influences host specificity in avian malaria parasites. Ecol. Lett. 22, 547–557. https://doi.org/10.1111/ele.13215.

Fick, S.E., Hijmans, R.J., 2017. WorldClim 2: new 1-km spatial resolution climate surfaces for global land areas. Int. J. Climatol. 37, 4302–4315. https://doi.org/10.1002/joc.5086.

Filion, A., Eriksson, A., Jorge, F., Niebuhr, C.N., Poulin, R., 2020. Large-scale disease patterns explained by climatic seasonality and host traits. Oecologia 194, 723–733. https://doi.org/10.1007/s00442-020-04782-x.

Fischer, S.E., 2020. Post-fledging and migration ecology of gray vireos (*Vireo vicinior*) and using ArtScience to explore gender and identity. Master's thesis, The University of Toledo, Toledo, OH, USA. https://doi.org/10.13140/RG.2.2.31260.41603.

Fischer, S.E., Granillo, K., Streby, H.M., 2022. Post-fledging survival, movements, and habitat associations of gray vireos in New Mexico. Avian Conserv. Ecol. 17, art13. https://doi.org/10.5751/ACE-02053-170113.

Fischer, S.E., Kramer, G.R., Baumann, M.J., Fahy, E.F., Granillo, K., Streby, H.M., 2025. Migratory connectivity and potential nonbreeding sexual segregation in Gray Vireos (*Vireo vicinior*). Wilson J. Ornithol. https://doi.org/10.1080/15594491.2025.2497654.

Fox, J., Weisberg, S., 2019. An R companion to applied regression, Third. ed. Sage, Thousand Oaks, CA.

765 Freeman, B. G., Class Freeman, A. M., Hochachka, W. M., 2016. Asymmetric interspecific
766 aggression in New Guinean songbirds that replace one another along an elevational gradient.
767 Ibis 158(4), 726–737. https://doi.org/10.1111/ibi.12384.
768 Gage K.L., Burkot T.R., Eisen R.J., Hayes, E.B.,. 2008. Climate and vectorborne diseases. Am. J.
769 Prev. Med. 35, 436–450. https://doi.org/10.1016/j.amepre.2008.08.030.
770 Galen, S.C., Borner, J., Martinsen, E.S., Schaer, J., Austin, C.C., West, C.J., Perkins, S.L., 2018.
771 The polyphyly of *Plasmodium*: comprehensive phylogenetic analyses of the malaria
772 parasites (order Haemosporida) reveal widespread taxonomic conflict. R. Soc. Open Sci. 5,
773 171780. https://doi.org/10.1098/rsos.171780.
774 Galen, S.C., Witt, C.C., 2014. Diverse avian malaria and other haemosporidian parasites in Andean
775 house wrens: evidence for regional co-diversification by host-switching. J. Avian Biol. 45,
776 374–386. https://doi.org/10.1111/jav.00375.
777 González, A.D., Matta, N.E., Ellis, V.A., Miller, E.T., Ricklefs, R.E., Gutiérrez, H.R., 2014. Mixed
778 species flock, nest height, and elevation partially explain avian haemoparasite Prevalence in
779 Colombia. PLOS ONE 9, e100695. https://doi.org/10.1371/journal.pone.0100695.
780 Granthon, C., Williams, D.A., 2017. Avian malaria, body condition, and blood parameters in four
781 species of songbirds. Wilson J. Ornithol. 129, 492–508. https://doi.org/10.1676/16-060.1
782 Gyllenhaal, E.F., 2024. Crossing the ocean: the importance of gene flow in island evolution.
783 University of New Mexico, Albuquerque, NM, USA.
784 Hackett, S.J., Kimball, R.T., Reddy, S., Bowie, R.C.K., Braun, E.L., Braun, M.J., Chojnowski, J.L.,
785 Cox, W.A., Han, K.-L., Harshman, J., Huddleston, C.J., Marks, B.D., Miglia, K.J., Moore,
786 W.S., Sheldon, F.H., Steadman, D.W., Witt, C.C., Yuri, T., 2008. A phylogenomic study of
787 birds reveals their evolutionary history. Science 320, 1763–1767.
788 https://doi.org/10.1126/science.1157704.

789 Hasik, A.Z., Siepielski, A.M., 2022. Parasitism shapes selection by drastically reducing host fitness
790 and increasing host fitness variation. Biol. Lett. 18, 20220323.
791 https://doi.org/10.1098/rsbl.2022.0323.
792 Hellgren, O., Waldenström, J., Bensch, S., 2004. A new PCR assay for simultaneous studies of
793 *Leucocytozoon*, *Plasmodium*, and *Haemoproteus* from avian blood. J. Parasitol. 90, 797–
794 802.
795 Hellgren, O., Waldenström, J., Peréz-Tris, J., Szöll, E., Si, Ö., Hasselquist, D., Krizanauskiene, A.,
796 Ottosson, U., Bensch, S., 2007. Detecting shifts of transmission areas in avian blood
797 parasites — a phylogenetic approach. Mol. Ecol. 16, 1281–1290.
798 https://doi.org/10.1111/j.1365-294X.2007.03227.x.
799 Hsieh, T.C., Ma, K.H., Chao, A., 2024. iNEXT: iNterpolation and EXTrapolation for species
800 diversity.
801 Huang, X., Jönsson, J., Bensch, S., 2020. Persistence of avian haemosporidians in the wild: a case
802 study to illustrate seasonal infection patterns in relation to host life stages. Int. J. Parasitol.
803 50, 611–619. https://doi.org/10.1016/j.ijpara.2020.05.006.
804 Hubbard, J.P., 1970. Check-list of the birds of New Mexico. N. M. Ornithol. Soc. 3, 108.
805 Illera, J.C., López, G., García-Padilla, L., Moreno, Á., 2017. Factors governing the prevalence and
806 richness of avian haemosporidian communities within and between temperate mountains.
807 PLOS ONE 12, e0184587. https://doi.org/10.1371/journal.pone.0184587.
808 Ikemoto T., 2008. Tropical malaria does not mean hot environments. J. Med. Entomol. 45(6), 963–
809 969.
810 Ishtiaq, F., Barve, S., 2018. Do avian blood parasites influence hypoxia physiology in a high
811 elevation environment? BMC Ecol. 18. https://doi.org/10.1186/s12898-018-0171-2.
812 Jetz, W., Thomas, G.H., Joy, J.B., Hartmann, K., Mooers, A.O., 2012. The global diversity of birds
813 in space and time. Nature 491, 444–498. https://doi.org/10.1038/nature11631.

Kassambara, A., 2023. rstatix: Pipe-friendly framework for basic statistical tests. R package version 0.7.2. https://CRAN.R-project.org/package=rstatix.

Kearse, M., Moir, R., Wilson, A., Stones-Havas, S., Cheung, M., Sturrock, S., Buxton, S., Cooper, A., Markowitz, S., Duran, C., Thierer, T., Ashton, B., Meintjes, P., Drummond, A., 2012. Geneious basic: An integrated and extendable desktop software platform for the organization and analysis of sequence data. Bioinformatics 28, 1647–1649. https://doi.org/10.1093/bioinformatics/bts199.

Kim, K.S., Tsuda, Y., 2010. Seasonal changes in the feeding pattern of *Culex pipiens pallens* govern the transmission dynamics of multiple lineages of avian malaria parasites in Japanese wild bird community: vector study of avian malaria transmission. Mol. Ecol. 19, 5545–5554. https://doi.org/10.1111/j.1365-294X.2010.04897.x.

Krasnov, B.R. and Poulin, R., 2010. Ecological properties of a parasite: species-specific stability and geographical variation. The biogeography of host–parasite interactions. Oxford University Press, Oxford, pp. 99-113.

Kuhn, M., 2008. Building Predictive Models in *R* Using the caret Package. J. Stat. Softw. 28. https://doi.org/10.18637/jss.v028.i05.

Kushary, D., 2000. Bootstrap methods and their application. Technometrics 42, 216–217. https://doi.org/10.1080/00401706.2000.10486018.

LaPointe, D.A., Atkinson, C.T., Samuel, M.D., 2012. Ecology and conservation biology of avian malaria. Ann. N. Y. Acad. Sci. 1249, 211–226. https://doi.org/10.1111/j.1749-6632.2011.06431.x.

Lauron, E.J., Loiseau, C., Bowie, R.C.K., Spicer, G.S., Smith, T.B., Melo, M., Sehgal, R.N.M., 2015. Coevolutionary patterns and diversification of avian malaria parasites in African sunbirds (Family Nectariniidae). Parasitology 142, 635–647. https://doi.org/10.1017/S0031182014001681.

Lele, S.R., Keim, J.L., Solymos, P., 2023. ResourceSelection: resource selection (probability) functions for use-availability data. https://CRAN.R-project.org/package=ResourceSelection.

Loiseau, C., Harrigan, R.J., Bichet, C., Julliard, R., Garnier, S., Lendvai, Á.Z., Chastel, O., Sorci, G., 2013. Predictions of avian *Plasmodium* expansion under climate change. Sci. Rep. 3, 1126. https://doi.org/10.1038/srep01126.

Lutz, H.L., Hochachka, W.M., Engel, J.I., Bell, J.A., Tkach, V.V., Bates, J.M., Hackett, S.J., Weckstein, J.D., 2015. Parasite prevalence corresponds to host life history in a diverse assemblage of Afrotropical birds and haemosporidian parasites. PLOS ONE 10, e0121254. https://doi.org/10.1371/journal.pone.0121254.

Mangiafico, S.S., 2024. rcompanion: Functions to Support Extension Education Program Evaluation. R package version 2.4.36. https://CRAN.R-project.org/package=rcompanion.

Marroquin-Flores, R.A., Williamson, J.L., Chavez, A.N., Bauernfeind, S.M., Baumann, M.J., Gadek, C.R., Johnson, A.B., McCullough, J.M., Witt, C.C., Barrow, L.N., 2017. Diversity, abundance, and host relationships in the avian malaria community of New Mexico pine forests. PeerJ 5, e3700–e3700. https://doi.org/10.7717/peerj.3700.

McNew, S.M., Barrow, L.N., Williamson, J.L., Galen, S.C., Skeen, H.R., DuBay, S.G., Gaffney, A.M., Johnson, A.B., Bautista, E., Ordoñez, P., Schmitt, C.J., Smiley, A., Valqui, T., Bates, J.M., Hackett, S.J., Witt, C.C., 2021. Contrasting drivers of diversity in hosts and parasites across the tropical Andes. Proc. Natl. Acad. Sci. 118, e2010714118. https://doi.org/10.1073/pnas.2010714118.

Medeiros, M.C.I., Hamer, G.L., Ricklefs, R.E., 2013. Host compatibility rather than vector–host-encounter rate determines the host range of avian *Plasmodium* parasites. Proc. R. Soc. B Biol. Sci. 280, 20122947. https://doi.org/10.1098/rspb.2012.2947.

Minchella, D.J., Scott, M.E., 1991. Parasitism: A cryptic determinant of animal community structure. Trends Ecol. Evol. 6, 250–254. https://doi.org/10.1016/0169-5347(91)90071-5.

Mordecai, E. A., Paaijmans, K. P., Johnson, L. R., Balzer, C., Ben-Horin, T., De Moor, E., McNally, A., Pawar, S., Ryan, S. J., Smith, T. C., & Lafferty, K. D., 2013. Optimal temperature for malaria transmission is dramatically lower than previously predicted. Ecol. Lett. 16(1), 22–30. https://doi.org/10.1111/ele.12015.

Mukhin, A., Palinauskas, V., Platonova, E., Kobylkov, D., Vakoliuk, I., Valkiūnas, G., 2016. The strategy to survive primary malaria infection: an experimental study on behavioural changes in parasitized birds. PLOS ONE 11, e0159216. https://doi.org/10.1371/journal.pone.0159216.

Muriel, J., 2020. Ecophysiological assessment of blood haemosporidian infections in birds. Ecosistemas 29. https://doi.org/10.7818/ecos.1979.

Names, G.R., Schultz, E.M., Krause, J.S., Hahn, T.P., Wingfield, J.C., Heal, M., Cornelius, J.M., Klasing, K.C., Hunt, K.E., 2021. Stress in paradise: effects of elevated corticosterone on immunity and avian malaria resilience in a Hawaiian passerine. J. Exp. Biol. 224. https://doi.org/10.1242/jeb.242951.

Oakgrove, K.S., Harrigan, R.J., Loiseau, C., Guers, S., Seppi, B., Sehgal, R.N.M., 2014. Distribution, diversity and drivers of blood-borne parasite co-infections in Alaskan bird populations. Int. J. Parasitol. 44, 717–727. https://doi.org/10.1016/j.ijpara.2014.04.011.

Pérez-Rodríguez, A., Fernández-González, S., De La Hera, I., Pérez-Tris, J., 2013. Finding the appropriate variables to model the distribution of vector-borne parasites with different environmental preferences: climate is not enough. Glob. Change Biol. 19, 3245–3253. https://doi.org/10.1111/gcb.12226.

Perkins, S.L., 2014. Malaria's many mates: past, present, and future of the systematics of the order Haemosporida. J. Parasitol. 100, 11–25. https://doi.org/10.1645/13-362.1.

Pigeault, R., Chevalier, M., Cozzarolo, C.S., Baur, M., Arlettaz, M., Cibois, A., Keiser, A., Guisan, A., Christe, P., Glaizot, O., 2022. Determinants of haemosporidian single- and co-infection

risks in western palearctic birds. Int. J. Parasitol. 52, 617–627. https://doi.org/10.1016/j.ijpara.2022.05.002.

Poulin, R., 2011. Evolutionary ecology of parasites. Princeton University Press, Princeton, New Jersey.

Poulin, R., Krasnov, B. R., 2010. Similarity and variability of parasite assemblages across geographical space. The biogeography of host–parasite interactions. Oxford University Press, Oxford, pp. 115-127.

R Core Team, 2023. R: A language and environment for statistical computing. R Foundation for Statistical Computing, Vienna, Austria. URL https://www.R-project.org/.

Reinoso-Pérez, M.T., Dhondt, K.V., Dulcet, H., Katzenstein, N., Sydenstricker, A.V., Dhondt, A.A., 2024. Seasonal variation in detection of Haemosporidia in a bird community: a comparison of nested PCR and microscopy. J. Wildl. Dis. 60. https://doi.org/10.7589/JWD-D-23-00023.

Ricklefs, R.E., Fallon, S.M., 2002. Diversification and host switching in avian malaria parasites. Proc. R. Soc. Lond. B Biol. Sci. 269, 885–892. https://doi.org/DOI 10.1098/rspb.2001.1940.

Ricklefs, R.E., Fallon, S.Y.M., Bermingham, E., 2004. Evolutionary relationships, cospeciation, and host switching in avian malaria parasites. Syst. Biol. 53.

Rodriguez, M.D., Doherty, P.F., Piaggio, A.J., Huyvaert, K.P., 2021. Sex and nest type influence avian blood parasite prevalence in a high-elevation bird community. Parasit. Vectors 14, 145. https://doi.org/10.1186/s13071-021-04612-w.

Rodríguez-Hernández, K., Álvarez-Mendizábal, P., Chapa-Vargas, L., Escobar, F., González-García, F., Santiago-Alarcon, D., 2021. Haemosporidian prevalence, parasitaemia and aggregation in relation to avian assemblage life history traits at different elevations. Int. J. Parasitol. 51, 365–378. https://doi.org/10.1016/j.ijpara.2020.10.006.

Santiago-Alarcon, D., Palinauskas, V., Schaefer, H.M., 2012. Diptera vectors of avian Haemosporidian parasites: untangling parasite life cycles and their taxonomy. Biol. Rev. 87, 928–964. https://doi.org/10.1111/j.1469-185X.2012.00234.x.

Schrader, M.S., Walters, E.L., James, F.C., Greiner, E.C., 2003. Seasonal prevalence of a haemotozoan parasite of red-bellied woodpeckers (*Melanerpes carolinus*) and its association with host condition and overwinter survival. The Auk 120, 130. https://doi.org/10.1642/0004-8038.

Sheppard, P., Comrie, A., Packin, G., Angersbach, K., Hughes, M., 2002. The climate of the US Southwest. Clim. Res. 21, 219–238. https://doi.org/10.3354/cr021219.

Sibley, C.G., Monroe, J., 1990. Distribution and taxonomy of birds of the world. Yale University Press, New Haven, CT.

Slowinski, S.P., Geissler, A.J., Gerlach, N., Heidinger, B.J., Ketterson, E.D., 2022. The probability of being infected with haemosporidian parasites increases with host age but is not affected by experimental testosterone elevation in a wild songbird. J. Avian Biol. 2022, jav.02819. https://doi.org/10.1111/jav.02819.

Stamatakis, A., 2014. RAxML version 8: a tool for phylogenetic analysis and post-analysis of large phylogenies. Bioinformatics 30, 1312–1313. https://doi.org/10.1093/bioinformatics/btu033.

Stöver, B.C., Müller, K.F., 2010. TreeGraph 2: combining and visualizing evidence from different phylogenetic analyses. BMC Bioinformatics 11, 7. https://doi.org/10.1186/1471-2105-11-7.

Sundar D., 2006. binom: Binomial confidence intervals for several parameterizations. R package version 1.1-1.1. https://CRAN.R-project.org/package=binom.

Tang, Y., Horikoshi, M., Li, W., 2016. ggfortify: Data visualization tools for statistical analysis results. https://CRAN.R-project.org/package=ggfortify.

Valkiūnas, G., 2005. Avian malaria parasites and other Haemosporidia, 1st ed. CRC Press, Boca Raton.

von Humboldt A., Bonpland A., 2009. Essay on the geography of plants—with a physical tableau of the equinoctial regions (1807). In: Jackson ST (ed) Essay on the geography of plants. University of Chicago Press, Chicago, pp 61–155.

Waldenström, A.J., Bensch, S., Hasselquist, D., Östman, Ö., Pryor, G.S., Greiner, E.C., Hall, B., 2004. A new nested polymerase chain reaction method very efficient in detecting Plasmodium and Haemoproteus infections from avian blood. J. Parasitol. 90, 191–194. https://doi.org/10.1645/GE-3221RN.

Walther, E.L., Carlson, J.S., Cornel, A., Morris, B.K., Sehgal, R.N.M., 2016. First molecular study of prevalence and diversity of avian haemosporidia in a Central California songbird community. J. Ornithol. 157, 549–564. https://doi.org/10.1007/s10336-015-1301-7.

Wickham, H., 2016. ggplot2, Use R! Springer International Publishing, Cham. https://doi.org/10.1007/978-3-319-24277-4.

Williamson, J.L., Witt, C.C., 2021. Elevational niche-shift migration: Why the degree of elevational change matters for the ecology, evolution, and physiology of migratory birds. Ornithology 138, ukaa087. https://doi.org/10.1093/ornithology/ukaa087.

Williamson, J.L., Wolf, C.J., Barrow, L.N., Baumann, M.J., Galen, S.C., Schmitt, C.J., Schmitt, D.C., Winter, A.S., Witt, C.C., 2019. Ecology, not distance, explains community composition in parasites of sky-island Audubon's Warblers. Int. J. Parasitol. 49, 437–448. https://doi.org/10.1016/j.ijpara.2018.11.012.

Wyckoff, S.T., Judkins, T.C., Nemeth, N.M., Ruder, M.G., Martin, J.A., Kunkel, M.R., Garrett, K.B., Adcock, K.G., Mead, D.G., Yabsley, M.J., 2024. Surveillance for selected pathogens and parasites of northern bobwhite (*Colinus virginianus*) from western Oklahoma, USA. 2018–20. J. Wildl. Dis. 60. https://doi.org/10.7589/jwd-d-23-00102.

Zamora-Vilchis, I., Williams, S. E., & Johnson, C. N., 2012. Environmental temperature affects prevalence of blood parasites of birds on an elevation gradient: implications for disease in a warming climate. PLOS ONE 7(6), e39208. https://doi.org/10.1371/journal.pone.0039208

## DATA STATEMENT

Specimen and parasite data are available in Supplementary Tables S1–S11 and are searchable via Arctos (arctos.database.museum; Cicero et al., 2024). Parasite sequences are archived in GenBank (accession nos. PV295634-PV295830). Vouchered specimens and frozen tissue samples are archived at the Museum of Southwestern Biology Division of Birds and Division of Genomic Resources, respectively, where they are available for further study (https://msb.unm.edu/). All R code and datasets are available on FigShare (https://doi.org/10.6084/m9.figshare.28585943).

## CONFLICT OF INTEREST STATEMENT

The authors have no conflicts of interest to declare.

## ETHICS STATEMENT

Research activities were conducted under Institutional Animal Care and Use Protocol 16-200406-MC and appropriate state and federal scientific collecting permits (New Mexico Department of Game and Fish Authorization Number 3217; US Fish and Wildlife Permit Numbers MB094297-0 and MB0942970-1).

## FUNDING STATEMENT

This work was supported by the National Science Foundation (Graduate Research Fellowship NSF-DGE-2439853 to DLFW; Postdoctoral Research Fellowship in Biology NSF-DBI-1611710 to LNB; and NSF-DEB-1146491 to CCW), the Bureau of Land Management Rio Puerco Field Office (via the Colorado Plateau Cooperative Eco-systems Studies Unit agreement), New Mexico Department of Game and Fish Share with Wildlife Grant to HMS/SEF, and a Sevilleta LTER Graduate Summer Research Fellowship and New Mexico Ornithological Society Ryan Beaulieu Research Grant to SEF.

990 TABLES

| ***Top five infection probability fixed effects additive models*** | | | | | |
|---|---|---|---|---|---|
| Bell's Vireo (*n* = 20) | | | | | |
| *Rank* | *Predictors* | *K* | *AICc* | *ΔAICc* | *Weight* |
| *1* | tempPC2 + precipPC1 | 3 | 22.6 | - | 0.324 |
| *2* | tempPC1 | 2 | 23.6 | *0.967* | 0.200 |
| *3* | precipPC1 | 2 | 24.7 | *0.348* | 0.113 |
| *4* | tempPC1 + precipPC1 | 3 | 25.9 | *0.199* | 0.064 |
| *5* | Elevation + tempPC1 | 3 | 25.9 | *0.197* | 0.064 |
| Gray Vireo (*n* = 170) | | | | | |
| *Rank* | *Predictors* | *K* | *AICc* | *ΔAICc* | *Weight* |
| *1* | Elevation + tempPC1 | 3 | 204 | - | 0.419 |
| *2* | Elevation + precipPC1 + tempPC1 | 4 | 206 | *1.72* | 0.177 |
| *3* | Elevation + precipPC2 + tempPC1 | 4 | 206 | *1.73* | 0.177 |
| *4* | Elevation + tempPC1 + tempPC2 | 4 | 206 | *2.07* | 0.149 |
| *5* | Elevation + tempPC1 + tempPC2, precipPC1 + precipPC2 | 5 | 207 | *3.35* | 0.078 |
| Plumbeous Vireo (*n* = 58) | | | | | |
| *Rank* | *Predictors* | *K* | *AICc* | *ΔAICc* | *Weight* |
| *1* | Null model | 1 | 52.1 | - | 0.301 |
| *2* | precipPC2 | 2 | 52.4 | *0.409* | 0.246 |
| *3* | precipPC1 | 2 | 53.3 | *1.17* | 0.168 |
| *4* | tempPC2 | 2 | 53.4 | *1.29* | 0.158 |
| *5* | PrecipPC1 + precipPC2 | 2 | 53.9 | *1.73* | 0.127 |

991 **Table 1. Top five models assessing environmental predictors of haemosporidian infection for**

992 **each species.** Sample sizes for datasets and directionality of best model outputs are listed at the top.

993 Models were ranked by AICc, with ΔAICc values relative to the top model and corresponding

994 Akaike weights (Weight) indicating model support.

995

| | Bell's Vireo top models | | | | Gray Vireo top models | | | | Plumbeous Vireo top models | | | |
|---|---|---|---|---|---|---|---|---|---|---|---|---|
| | Model-averaged estimate and 95% confidence limits | | | | Model-averaged estimate and 95% confidence limits | | | | Model-averaged estimate and 95% confidence limits | | | |
| **Parameter** | **β** | **SE** | **Lower CL** | **Upper CL** | **β** | **SE** | **Lower CL** | **Upper CL** | **β** | **SE** | **Lower CL** | **Upper CL** |
| Intercept | 0.845 | 0.876 | -0.989 | 2.68 | 1.14 | 0.357 | 0.433 | 1.84 | 1.74 | 0.377 | 0.983 | 2.49 |
| Elevation | 0.062 | 0.371 | -0.703 | 0.827 | -1.72 | 0.763 | -3.23 | -0.214 | - | - | - | - |
| tempPC1 | -0.938 | 1.44 | -3.85 | 1.98 | 1.08 | 0.546 | 0.006 | 2.16 | - | - | - | - |
| tempPC2 | 1.80 | 2.65 | -3.54 | 7.14 | -0.048 | 0.717 | -1.46 | 1.37 | 0.051 | 0.179 | -0.305 | 0.406 |
| precipPC1 | 2.83 | 3.47 | -4.15 | 9.80 | -0.163 | 0.588 | -1.32 | 0.996 | 0.099 | 0.24 | -0.378 | 0.577 |
| precipPC2 | NA | NA | NA | NA | -0.278 | 0.901 | -2.05 | 1.50 | 0.172 | 0.309 | -0.439 | 0.783 |

997 **Table 2. Standardized model-averaged regression coefficients used to estimate effects of**
998 **predictors and precision of effects across species-specific candidate model sets that assess**
999 **environmental predictors of haemosporidian infection.** Regression coefficients (β), standard
1000 error (SE), and 95% confidence limits (CL) are given. Dashes indicate that the parameter was not
1001 present in a final model set, and NA values indicate that the parameter was not tested due to lack of
1002 variation present in model set.
1003

1004 FIGURES

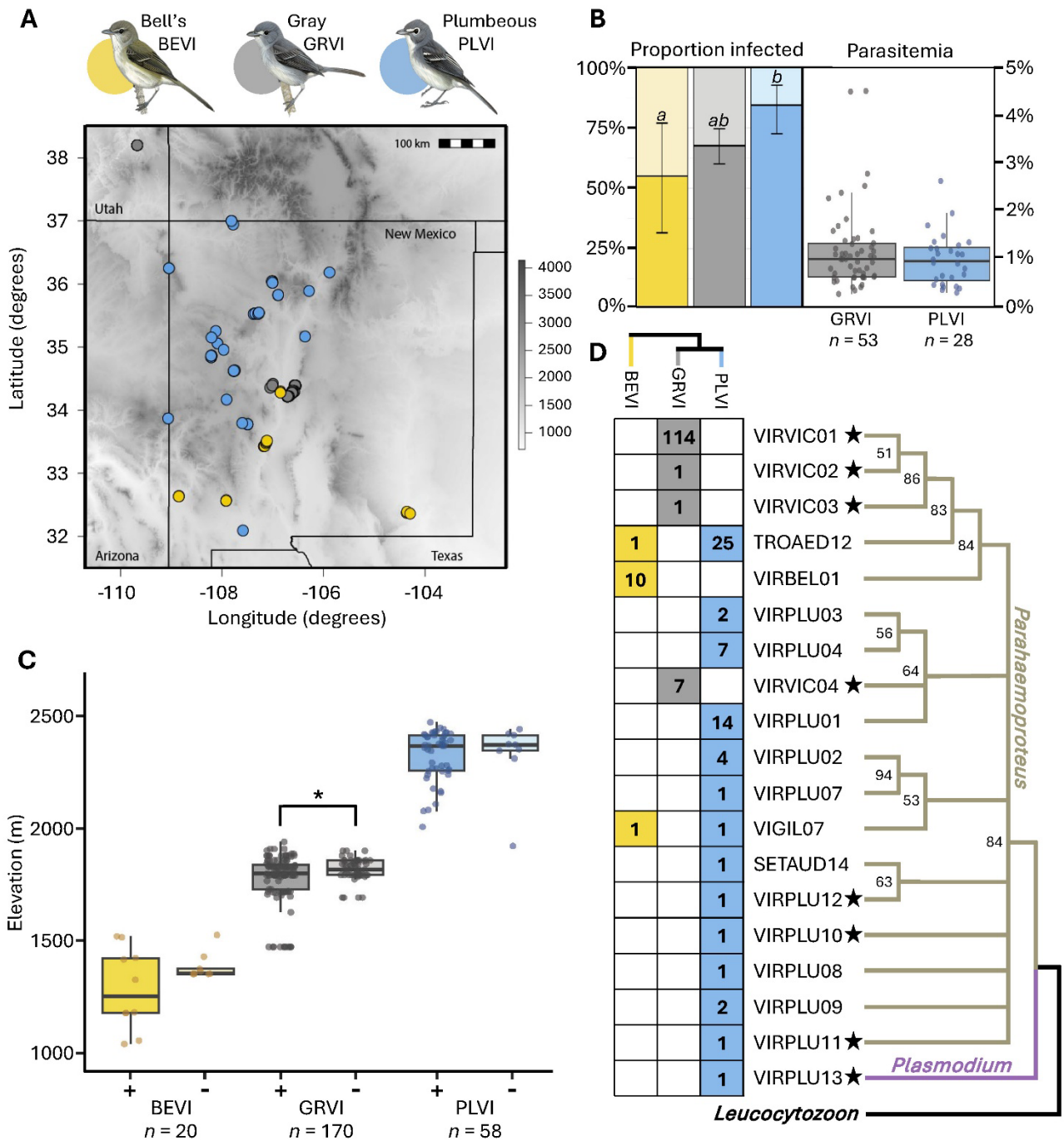


1005

1006 **Figure 1)** A) Sampling distribution for each host species (Bell's Vireo: *Vireo bellii,* Gray Vireo: *V.*
1007 *vicinior,* and Plumbeous Vireo: *V. plumbeus*) in the southwestern USA; B) Left: summary of
1008 infection prevalence, with significant differences between groups determined using multiple
1009 Pearson chi-squared tests and Bonferroni-corrected p-values indicated by letters. Error bars
1010 represent 95% confidence intervals for positive infection proportions. Right: percent parasitemia for
1011 Gray and Plumbeous vireos. C) Proportion of individuals infected versus uninfected across the

1012 sampled elevational gradient. Asterisk denotes significant p-values (< 0.05) based on Mann-
1013 Whitney U-tests; D) Phylogeny of 19 haemosporidian cyt *b* haplotypes and their respective
1014 abundances per species. Stars denote novel haplotypes and bootstrap values >50 are shown at
1015 nodes. Bird images courtesy Birds of the World (Billerman et al., 2025).
1016

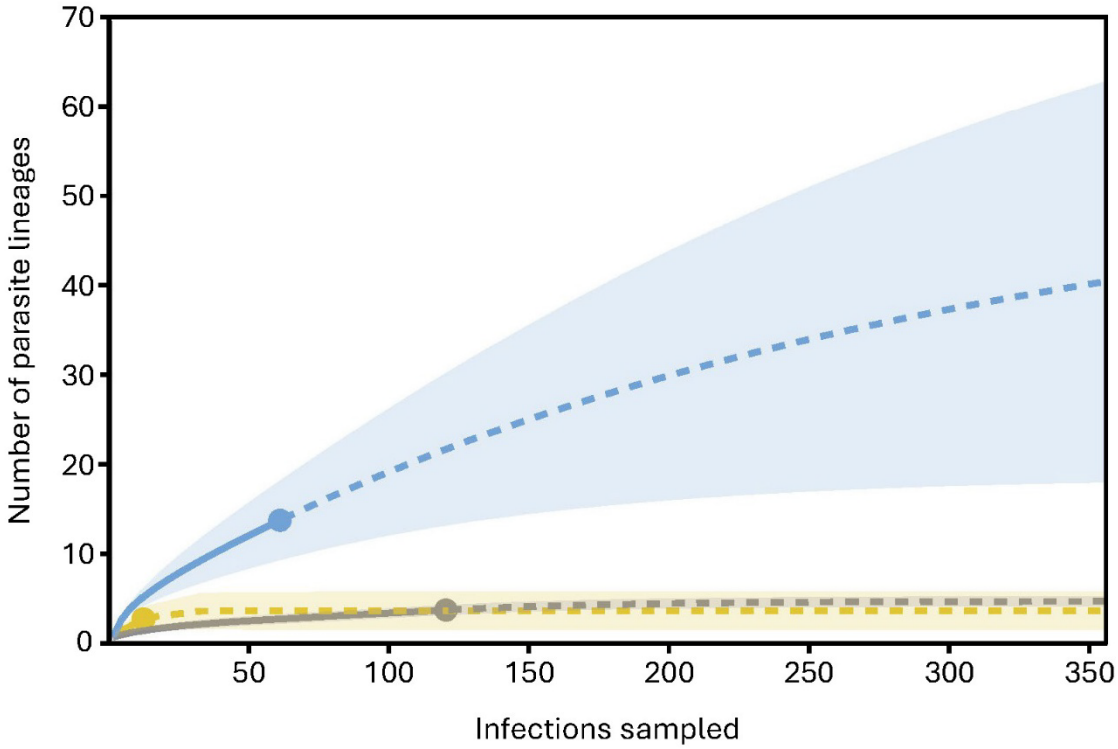


1017

1018 **Figure 2)** Estimate of haemosporidian lineage diversity in Bell's (*Vireo belli*), Gray (*V. vicinior*)
1019 and Plumbeous Vireos (*V. plumbeus*) based on iNEXT rarefaction and extrapolation. Bell's Vireos
1020 curves, shown in yellow, were created using 12 avian haemosporidian infections and three
1021 haplotypes; Gray Vireo curves, shown in gray, were created using 123 avian haemosporidian
1022 infections and four haplotypes; Plumbeous Vireo curves, shown in blue, used 62 haemosporidian
1023 infections and 14 haplotypes. Points indicate the reference sample, solid line the rarefaction
1024 estimate, and dotted line the extrapolation. The analysis suggested that sampling approximately 33
1025 total infections in Bell's, 14 total infections for Gray, and 364 total infections for Plumbeous Vireos
1026 would capture >95% of the haemosporidian lineage diversity in this community. The total

haplotype richness, rounded to nearest whole number, is estimated to be four for Bell's Vireos (95% CI [3-6]), five for Gray Vireos (95% CI [4 – 6]) and 54 for Plumbeous Vireos (95% CI [14 – 101]).

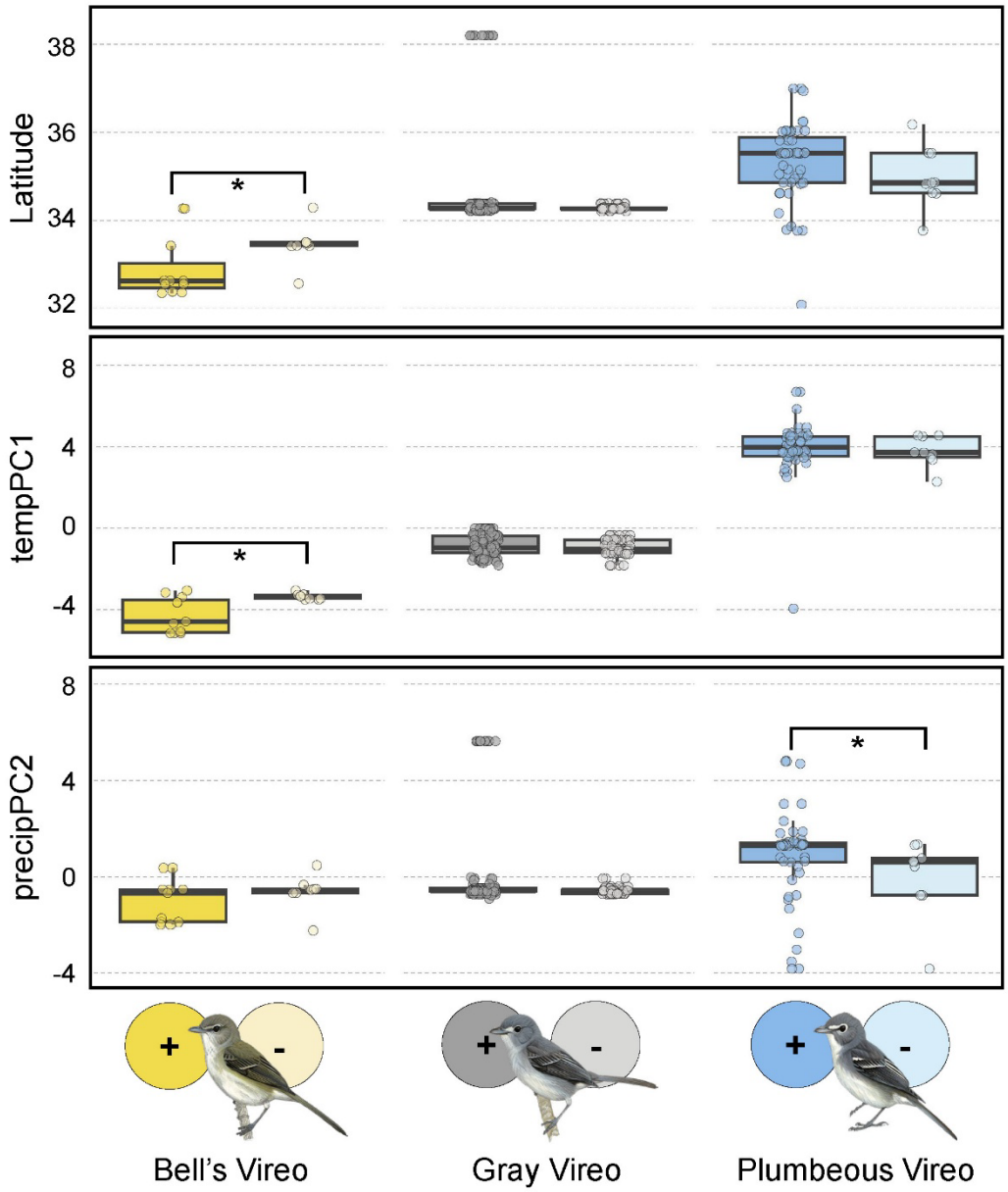


**Figure 3)** Intraspecific distribution of infected and uninfected vireos across associated environmental variables. Higher tempPC1 values relate to cooler overall temperatures and higher precipPC2 relates to sites with more seasonally stable precipitation. Significantly different distributions, determined by Mann-Whitney U-tests are denoted by an asterisk ($p < 0.05$).